

Uniqueness and reconstruction in magnetic resonance–electrical impedance tomography (MR–EIT)

Y Ziya İder¹, Serkan Onart¹ and William R B Lionheart²

¹ Department of Electrical and Electronics Engineering, Bilkent University, Ankara, Turkey

² Department of Mathematics, UMIST, UK

E-mail: ıder@ee.bilkent.edu.tr

Received 18 October 2002

Published 30 April 2003

Online at stacks.iop.org/PM/24/591

Abstract

Magnetic resonance–electrical impedance tomography (MR–EIT) was first proposed in 1992. Since then various reconstruction algorithms have been suggested and applied. These algorithms use peripheral voltage measurements and internal current density measurements in different combinations. In this study the problem of MR–EIT is treated as a hyperbolic system of first-order partial differential equations, and three numerical methods are proposed for its solution. This approach is not utilized in any of the algorithms proposed earlier. The numerical solution methods are integration along equipotential surfaces (method of characteristics), integration on a Cartesian grid, and inversion of a system matrix derived by a finite difference formulation. It is shown that if some uniqueness conditions are satisfied, then using at least two injected current patterns, resistivity can be reconstructed apart from a multiplicative constant. This constant can then be identified using a single voltage measurement. The methods proposed are direct, non-iterative, and valid and feasible for 3D reconstructions. They can also be used to easily obtain slice and field-of-view images from a 3D object. 2D simulations are made to illustrate the performance of the algorithms.

Keywords: Electrical impedance tomography, EIT, magnetic resonance–electrical impedance tomography, MR–EIT, medical imaging, image reconstruction, method of characteristics, hyperbolic system of partial differential equations

1. Introduction

Conventional injected current EIT uses boundary voltage data to reconstruct an image. It is known that this image is unique for noise-free complete boundary data (Sylvester and Uhlmann

1986). However, due to noise and low sensitivity of boundary voltages to inner conductivity perturbations, and also due to practical problems with electrodes which allow for only a limited number of boundary voltage measurements, conventional EIT can only yield inaccurate low resolution images. Magnetic resonance–electrical impedance tomography (MR–EIT) has been proposed to provide high resolution conductivity images by making use of an additional set of measurements which are made directly inside the object. These measurements can be made with high spatial sampling and also they have high sensitivity even to inner conductivity perturbations.

MR–EIT makes use of the measurement techniques developed for magnetic resonance current density imaging (MRCDI) (Scott *et al* 1991). In MRCDI, the magnetic field, \mathbf{H} , generated by the internal current distribution, \mathbf{J} , is measured using a magnetic resonance imaging system, and \mathbf{J} is obtained by $\mathbf{J} = \nabla \times \mathbf{H}$. MR–EIT then utilizes either \mathbf{J} or \mathbf{H} in addition to peripheral voltage measurements to obtain high resolution conductivity images. MR–EIT reconstruction algorithms fall into two categories; those making use of \mathbf{J} , and those making use of \mathbf{H} directly.

The concept of magnetic resonance–electrical impedance tomography (MR–EIT) was first introduced in 1992 by Zhang (1992) in his MSc thesis entitled ‘Electrical impedance tomography based on current density imaging’. Zhang developed an algorithm which is capable of reconstructing the correct image using internal current density and also the boundary voltage variation. His method is based on the fact that the voltage difference between any two points on the boundary is the integral of electrical field along any line connecting the two points. The electrical field is equal to $\rho\mathbf{J}$ where ρ is the resistivity, and since \mathbf{J} is measured, from different lines connecting the two points, and for different boundary point pairs, a linear system of equations can be obtained. Solution of this set of equations yields an image which is unique and correct. The method is valid for 3D reconstructions, as well as for single slice imaging. A drawback of this method is the requirement of many boundary voltage measurements to improve the accuracy and resolution of reconstruction.

Eyüboğlu *et al* (2002), Özdemir and Eyüboğlu (2002) and Kwon *et al* (2002b) have proposed algorithms based on constructing the equipotential lines in the object using peripheral voltages and current density distribution. Current density inside the object is measured and it is known that the equipotential lines and current lines are orthogonal. The potential and thus the electrical field distributions inside the object can be found by finding the equipotential lines and projecting the peripheral voltage measurements into the field of view (FOV) along these lines. Using the calculated electric field distribution and measured current density distribution, conductivity can be found for the entire FOV using Ohm’s law. These methods, similar to the method of Zhang (1992), are also non-iterative, and require peripheral voltage measurements and a single current injection pattern.

Woo *et al* (1994) have proposed a reconstruction algorithm whereby the error between the current density measured by MRCDI technique and the current density calculated by the finite-element method (FEM) is minimized as a function of the resistivity distribution. Kwon *et al* (2002a) have expanded on this idea to develop the ‘ J -substitution algorithm’, which uses (at least) two injected current patterns and a single voltage measurement to reconstruct the correct image. They also claim that at any point in the object, current densities measured for the two current injection patterns must not be parallel. This requirement of at least two injected current patterns is rigorously proved later by Kim *et al* (2002). Khang *et al* (2002) have applied the J -substitution algorithm successfully to data obtained from saline phantoms. Both methods in Woo *et al* (1994) and Kwon *et al* (2002a) are iterative. Another iterative method which is proposed by Eyuboglu *et al* (2001), is based on minimizing the error between measured and calculated current densities and peripheral voltages simultaneously. Recently

Birgöl *et al* (2003) have proposed another iterative method in which a single voltage measurement and eight current injection patterns are used. Their method is similar to the J -substitution method in concept, but they have also studied its performance under opposite drive and cosine injection patterns.

İder and Müftuler (1997) and İder and Birgöl (1998) have developed and applied to real data a method for reconstructing from the measured magnetic field without having to calculate the current density, using an iterative sensitivity matrix approach. Seo *et al* (2002) have also proposed a method which makes use of \mathbf{H} only. In both these methods only a single component of \mathbf{H} is used. This provides a major practical advantage over the methods utilizing \mathbf{J} because to obtain \mathbf{J} by taking the curl of \mathbf{H} requires the measurement of all three components of \mathbf{H} . Methods developed in this study are of the type utilizing \mathbf{J} , and therefore methods utilizing \mathbf{H} are not discussed further in this paper.

While developing a new reconstruction algorithm for MR-EIT (utilizing \mathbf{J}) the following questions are of interest:

- What combination of internal current density and boundary voltage measurements determines resistivity uniquely?
- To what extent can one make use of internal current density measurements alone?
- Is the algorithm stable against measurement noise?
- Is the algorithm applicable to 3D as well as 2D reconstructions?
- Is it an iterative or a direct (single run) algorithm?

In this study we have developed three new reconstruction algorithms for MR-EIT all of which are derived starting from $\nabla \times \rho \mathbf{J} = 0$ inside the object. The problem of reconstruction is treated as a hyperbolic system of first order partial differential equations, and the method of characteristics as well as two other numerical methods are used for solution. This approach is not utilized in any of the algorithms proposed earlier. We first address the problem of what can be reconstructed if current density measurements are used alone. We show that under certain conditions current density information is sufficient to reconstruct the correct image apart from a multiplicative factor. Then, in applications where the true resistivity distribution is required, we show that a single voltage measurement is enough to complete the picture. The three new reconstruction algorithms proposed in this study are 3D in nature, and they can easily be applied for slice and field-of-view imaging as well. Furthermore the methods are direct (non-iterative), and their uniqueness conditions are also established.

2. Derivation of the reconstruction algorithms

Let Ω be a connected and bounded domain in \mathbb{R}^3 , with boundary Γ , unit outward normal along Γ , \bar{n} , and positive conductivity σ . The resistivity $\rho = 1/\sigma$ is also assumed to be positive in Ω . Current is applied on part of Γ such that

$$\sigma \frac{\partial \phi}{\partial n} = \begin{cases} J_{\text{app}} & \text{on } \Gamma_2 \\ 0 & \text{on } \Gamma_1 \end{cases} \quad (1)$$

where J_{app} is the boundary injected current density, ϕ is the potential field in Ω (see figure 1 for a 2D illustration), and $\Gamma = \Gamma_1 \cup \Gamma_2$. A particular combination of Γ_1 , Γ_2 and J_{app} is called a ‘current injection pattern’ or simply an ‘injection pattern’.

It is assumed that current density in Ω is measured using MRCDI techniques (Scott *et al* 1991) and will be denoted as \mathbf{J} hereafter.

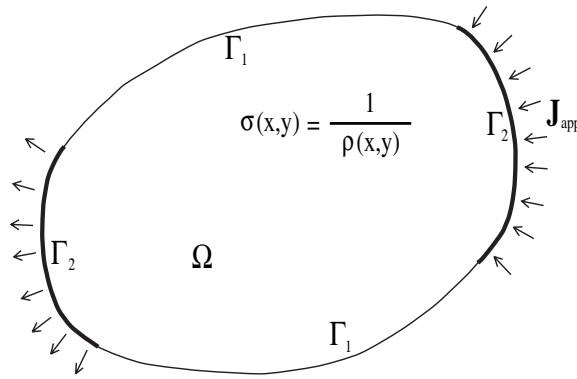


Figure 1. Illustration of the ‘injected current profile’ for a 2D resistive object.

Since static conditions are assumed

$$\nabla \times \mathbf{E} = 0 \text{ in } \Omega \quad (2)$$

where \mathbf{E} is the electric field in Ω . Since $\mathbf{E} = \rho \mathbf{J}$

$$\nabla \times \rho \mathbf{J} = 0 \quad (3)$$

and

$$\nabla \rho \times \mathbf{J} + \rho \nabla \times \mathbf{J} = 0. \quad (4)$$

Defining $R = \ln \rho$,

$$\nabla R \times \mathbf{J} = -\nabla \times \mathbf{J}. \quad (5)$$

Since \mathbf{J} is known, we can interpret this equation as yielding information on the gradient of R . To gain further insight about equation (5) let us expand its components in all directions to obtain the set of equations

$$\begin{bmatrix} 0 & J_z & -J_y \\ -J_z & 0 & J_x \\ J_y & -J_x & 0 \end{bmatrix} \begin{bmatrix} \frac{\partial R}{\partial x} \\ \frac{\partial R}{\partial y} \\ \frac{\partial R}{\partial z} \end{bmatrix} = - \begin{bmatrix} \frac{\partial J_z}{\partial y} - \frac{\partial J_y}{\partial z} \\ \frac{\partial J_x}{\partial z} - \frac{\partial J_z}{\partial x} \\ \frac{\partial J_y}{\partial x} - \frac{\partial J_x}{\partial y} \end{bmatrix} \quad (6)$$

or

$$\tilde{\mathbf{J}}^T \nabla R = -\nabla \times \mathbf{J} \quad (7)$$

where $\tilde{\mathbf{J}}$ is the transpose of the matrix on the left-hand side of (6). To be explicit

$$\tilde{\mathbf{J}} = [\tilde{\mathbf{J}}_1 \quad \tilde{\mathbf{J}}_2 \quad \tilde{\mathbf{J}}_3] \quad (8)$$

where

$$\tilde{\mathbf{J}}_1 = \begin{bmatrix} 0 \\ J_z \\ -J_y \end{bmatrix} \quad \tilde{\mathbf{J}}_2 = \begin{bmatrix} -J_z \\ 0 \\ J_x \end{bmatrix} \quad \text{and} \quad \tilde{\mathbf{J}}_3 = \begin{bmatrix} J_y \\ -J_x \\ 0 \end{bmatrix}.$$

Note that $\tilde{\mathbf{J}}_i \cdot \mathbf{J} = 0$ for $i = 1, 2, 3$.

2.1. Reconstruction by integration along equipotential lines—method of characteristics

2.1.1. Hyperbolic systems and uniqueness. The solution of a single first-order linear partial differential equation by the method of characteristics is a standard textbook technique (John

1982). We review the technique here before extending it to the case of a system of three equations as in (6).

For a vector field $\mathbf{A}(\mathbf{x})$ and scalar field $b(\mathbf{x})$, where $\mathbf{x} = [x \ y \ z]^T$, a first-order linear partial differential equation has the form

$$\mathbf{A} \cdot \nabla u = b. \tag{9}$$

A *characteristic curve* for this system is an integral curve $\mathbf{x}(s)$ with

$$\mathbf{x}'(s) = \mathbf{A}(\mathbf{x}(s)). \tag{10}$$

where $\mathbf{x}' = d\mathbf{x}/ds$. Therefore the characteristic curve passing through any point $\mathbf{x}(s_0)$, for which s is assigned to be s_0 , can be found by the integral

$$\mathbf{x}(s) = \mathbf{x}(s_0) + \int_{s_0}^s \mathbf{A}(\mathbf{x}(t)) \, dt. \tag{11}$$

We then have

$$\frac{d}{ds} u(\mathbf{x}(s)) = \nabla u \cdot \mathbf{x}'(s) = b(\mathbf{x}(s)) \tag{12}$$

and thus we can recover the solution u along the characteristic curve given its value at one point, say for $s = s_1$, on the curve from the integral

$$u(s) = u(s_1) + \int_{s_1}^s b(\mathbf{x}(t)) \, dt. \tag{13}$$

Given any *non-characteristic surface* S , i.e. a surface to which \mathbf{A} is not tangent anywhere, we can specify Cauchy data for this hyperbolic equation³ consisting of u restricted to S . These data are sufficient to determine u along all characteristic curves intersecting S .

Now each row of our system (6) is a first-order linear hyperbolic partial differential equation

$$\tilde{\mathbf{J}}_i \cdot \nabla R = -(\nabla \times \mathbf{J})_i \quad i = 1, 2, 3. \tag{14}$$

Taking the whole system of equations (6) together it constitutes a hyperbolic system. Note that the rank of $\tilde{\mathbf{J}}$ is two, for nonzero \mathbf{J} . At any given point the span of the columns of $\tilde{\mathbf{J}}$ is just the plane normal to \mathbf{J} and therefore this is the tangent plane at that point to an equipotential surface. The characteristic surfaces of the system (6) are therefore the equipotential surfaces. Cauchy data for this problem are the specification of R along a non-characteristic curve, that is a curve nowhere tangent to the family of equipotential surfaces, and the specification of R at any point on an equipotential determines R on the connected component of the equipotential surface containing that point. This can be achieved of course only for all equipotential surfaces intersecting the non-characteristic curve. The appendix explains how R can be determined in an equipotential surface if it is specified at one point in it.

Let us consider for simplicity the case where current is injected via a pair of point electrodes—a source and sink of current at the boundary Γ . For a simply connected domain Ω it is clear that the equipotential surfaces are connected, and that a curve in Ω joining the source and sink intersects every equipotential. One could, e.g., choose such a curve to be a current streamline, in which case it is orthogonal to each equipotential and intersects each exactly once. Specifying R at all points of this current streamline allows us to determine R at all equipotential surfaces and hence in all of Ω .

In order to see if R can be determined in all of Ω by specifying it at only one point, now consider two such current injection pairs with all four point electrodes different, for which the

³ It is a first-order partial differential equation so Cauchy data are zeroth derivatives.

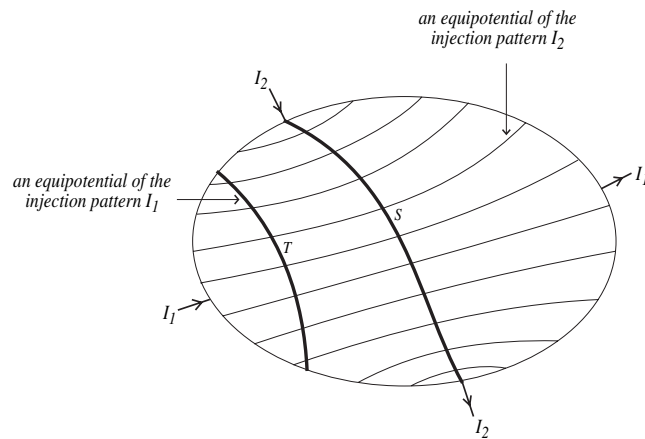


Figure 2. I_1 and I_2 denote two opposite current injection patterns which are applied one at a time. The dark solid lines S and T are two of the equipotentials corresponding to the I_1 injection pattern, and the other solid lines in the domain are the equipotentials corresponding to the I_2 injection pattern. The positions of the electrodes for the I_2 injection pattern are chosen to be at the ends of S which intersects all equipotentials of the I_2 injection pattern. Note that T does not intersect all equipotentials of the I_2 injection pattern.

interior current density is known (see figure 2 for a 2D illustration). Suppose we specify R at one point on an equipotential surface of the first injection pattern, S , and hence R is known on all of that equipotential surface. If S is a non-characteristic surface for the equipotentials of the second injection pattern we have that R is determined on all equipotentials for the second injection pattern intersecting S . However, for this example (i.e., two pairs of point current injections) we can choose the electrode positions so that the equipotentials of the second injection pattern intersecting S cover the entire domain Ω , e.g. if the second electrode pair lies on γ , where γ is the boundary where S intersects Γ . This selection of electrode positions is illustrated in figure 2. In this case, we see that R is determined completely by the interior current densities for two suitably chosen patterns up to one unknown constant. Consider now that R is specified on a point not on S . We can then move from this point along the corresponding equipotential of the second injection up to S , and then proceed to determine all of R in the whole domain.

The examples given above are simple cases which are used to illustrate some of the concepts. In order to derive conditions for uniqueness in general, let us again consider two injection patterns for which \mathbf{J}^1 and \mathbf{J}^2 are measured. If at a given point $\mathbf{J}^1 \times \mathbf{J}^2 \neq 0$, then the two equipotentials passing through that point corresponding to the two injection patterns are non-characteristic to each other, i.e. they are ‘not aligned’ or ‘transverse’ to each other. We call this condition the ‘transversality condition’. This allows us to move at that point from the equipotential of, for example, the first injection pattern, to its nearby equipotential by moving along the equipotential of the second injection. Thus if the transversality condition holds for at least one point on each equipotential of one of the injection patterns, then we can move in between any two equipotentials of that current injection. This is then sufficient to reconstruct R in all of Ω given its value at a single point. The transversality condition may not hold at a sufficient number of points by only two injection patterns, and therefore more than two injection patterns may be necessary so that for each equipotential of the first injection there is at least one second injection pattern such that the transversality condition holds on at least one point on each equipotential of the first injection. If this condition is still not met on a sufficient number of points then R can only be determined in the biggest set of points

which can be reached from the point at which it is specified by a chain of smooth curves each contained in the equipotential surface of one injection.

2.1.2. Slice imaging using the method of characteristics. Let us now concentrate on the third row of equation (6), which is

$$\frac{\partial R}{\partial x} J_y - \frac{\partial R}{\partial y} J_x = - \left(\frac{\partial J_y}{\partial x} - \frac{\partial J_x}{\partial y} \right) \quad (15)$$

or

$$\tilde{\mathbf{J}}_3 \cdot \nabla R = -(\nabla \times \mathbf{J})_3.$$

Note that this equation has characteristic curves defined by $\mathbf{x}'(s) = \tilde{\mathbf{J}}_3(\mathbf{x}(s))$ which stay in the same $z = \text{constant}$ plane as their starting points because $(\tilde{\mathbf{J}}_3)_3 = 0$. In fact the characteristic curve found for a starting point is the intersection of the $z = \text{constant}$ plane with the characteristic surface for the same point found by the hyperbolic system (6).

Consider a $z = c$ plane where c is a constant. Intersection of this plane with Ω is denoted by Ω_{xy}^c . In Ω_{xy}^c , $\left[\frac{\partial R}{\partial x} \frac{\partial R}{\partial y} \right]^T$ is the projection of the gradient of R on Ω_{xy}^c , and the left-hand side of equation (15) can be interpreted as the projection of this two-dimensional gradient on the $[J_y \ -J_x]^T$ direction which is perpendicular to the current direction $[J_x \ J_y]^T$. Thus the characteristic curves are perpendicular to current streamlines and are in fact the equipotential lines. Therefore R can be obtained in Ω_{xy}^c by integrating along the characteristic curves in Ω_{xy}^c provided R is known for at least one point in each characteristic curve.

Assume now that two different injected current patterns are used and two internal current density distributions \mathbf{J}^1 and \mathbf{J}^2 are measured. Let \mathbf{J}_{xy}^1 and \mathbf{J}_{xy}^2 be the projections of \mathbf{J}^1 and \mathbf{J}^2 in Ω_{xy}^c onto Ω_{xy}^c . If $\mathbf{J}_{xy}^1 \times \mathbf{J}_{xy}^2 \neq 0$ for at least one point on each equipotential line of one injection pattern, then, one needs to specify R on only a single point in Ω_{xy}^c . If this transversality condition holds for all points in Ω_{xy}^c the same conclusion can be drawn, but this is an over-specification.

Similarly one can obtain slice images for Ω_{yz}^c and Ω_{xz}^c using the first and second rows of (6), respectively.

2.2. Reconstruction by integration along Cartesian grid lines

For practical reasons integrations along a Cartesian grid may be preferred to integrations along equipotential lines.

If the gradient of a potential function is known in Ω , then that potential function can be found by integrating its gradient along Cartesian grid lines, except for an additive constant which is equivalent to specifying the potential function at a single point in Ω .

The determinant of the coefficient matrix in equation (6) is zero. Therefore the gradient of R cannot be found if a single injected current profile is employed. Let us then assume that there are two experimentally measured current densities \mathbf{J}^1 and \mathbf{J}^2 which correspond to two different injection patterns. The third row of equation (6) can then be written twice to obtain

$$\begin{bmatrix} J_y^1 & -J_x^1 \\ J_y^2 & -J_x^2 \end{bmatrix} \begin{bmatrix} \frac{\partial R}{\partial x} \\ \frac{\partial R}{\partial y} \end{bmatrix} = \begin{bmatrix} \frac{\partial J_y^1}{\partial x} - \frac{\partial J_x^1}{\partial y} \\ \frac{\partial J_y^2}{\partial x} - \frac{\partial J_x^2}{\partial y} \end{bmatrix}. \quad (16)$$

From this set of equations one can calculate $\left[\frac{\partial R}{\partial x} \frac{\partial R}{\partial y} \right]^T$ for any point (x, y, z) provided that for that point the determinant, $-J_y^1 J_x^2 + J_y^2 J_x^1$, is not zero, or equivalently

$$\mathbf{J}_{xy}^1 \times \mathbf{J}_{xy}^2 \neq 0, \quad (17)$$

where \mathbf{J}_{xy}^1 and \mathbf{J}_{xy}^2 are the projections of \mathbf{J}^1 and \mathbf{J}^2 onto the xy plane.

Once $\left[\frac{\partial R}{\partial x} \frac{\partial R}{\partial y}\right]^T$ is found, then, using the first or the second row of equation (6), one can find $\frac{\partial R}{\partial z}$ if at least one of the conditions $(J_y^1 \neq 0 \text{ or } J_y^2 \neq 0)$ or $(J_x^1 \neq 0 \text{ or } J_x^2 \neq 0)$ is satisfied, respectively. One of these conditions will hold anyway, because the condition in equation (17) is already required.

Handling the rows of equation (6) in different orders, one can show that to find the gradient of R at any point, it is also sufficient to have $(\mathbf{J}_{xz}^1 \times \mathbf{J}_{xz}^2) \neq 0$ or $(\mathbf{J}_{yz}^1 \times \mathbf{J}_{yz}^2) \neq 0$, at that point. In general if

$$\mathbf{J}^1 \times \mathbf{J}^2 = \mathbf{J}_{yz}^1 \times \mathbf{J}_{yz}^2 + \mathbf{J}_{xz}^1 \times \mathbf{J}_{xz}^2 + \mathbf{J}_{xy}^1 \times \mathbf{J}_{xy}^2 \neq 0 \quad (18)$$

at a certain point, then the gradient at that point can be calculated because at least one of the terms in (18) will not vanish. In practice one may need to employ more than two injection patterns because the condition in (18) may not be satisfied at all points by a single pair of injection patterns.

Note that by finding $\left[\frac{\partial R}{\partial x} \frac{\partial R}{\partial y}\right]^T$ for only one xy plane, one can reconstruct R at only that plane, i.e. slice, apart from an additive constant, without being concerned about finding the gradient at other xy slices. Similarly for xz and yz slices.

2.3. Reconstruction formulated as a linear set of equations using finite differences

Equation (15) can be discretized using finite differences for a rectangular mesh. For example for the third row of equation (6), and for the inner points central differences can be used

$$\begin{aligned} & \frac{1}{2\Delta x} [(R_{i+1,j} - R_{i-1,j})(J_y)_{i,j}] - \frac{1}{2\Delta y} [(R_{i,j+1} - R_{i,j-1})(J_x)_{i,j}] \\ &= - \left[\frac{1}{2\Delta x} ((J_y)_{i+1,j} - (J_y)_{i-1,j}) - \frac{1}{2\Delta y} ((J_x)_{i,j+1} - (J_x)_{i,j-1}) \right] \end{aligned} \quad (19)$$

where Δx and Δy are the discretization steps in the x and y directions, i and j are the indices of mesh element centres in the x and y directions and the index k representing z dependence is omitted for ease of representation. For points lying near the boundary of Ω , backward and/or forward differences can be used where appropriate. Rearranging the finite difference equations one can obtain a linear set of equations

$$\mathbf{CR} = \mathbf{B} \quad (20)$$

where $\mathbf{R} = [R_1, R_2, \dots, R_N]^T$ and N is the number of unknown logarithmic resistivities.

For M different injected current profiles, coefficient matrices and the right-hand side vectors can be concatenated to obtain the combined set of equations

$$\begin{bmatrix} \mathbf{C}_1 \\ \mathbf{C}_2 \\ \vdots \\ \mathbf{C}_M \end{bmatrix} \mathbf{R} = \begin{bmatrix} \mathbf{B}_1 \\ \mathbf{B}_2 \\ \vdots \\ \mathbf{B}_M \end{bmatrix}. \quad (21)$$

It must be noted of course that for any point (x, y, z) there must be at least two injected current profiles such that the condition expressed in equation (18) is satisfied. Still, the rank of this equation will be $N - 1$ because we know that, from its gradients, a function can be reconstructed only apart from an additional constant. Therefore one can specify one of the R 's and solve the reduced set of equations, to find the remaining R s.

Note again that this method can be used to obtain the logarithmic resistivities of only one slice without being concerned with other slices.

2.4. Need for a single voltage measurement

Using any of the reconstruction algorithms explained above, the correct $R(x, y, z)$ image can be reconstructed apart from an additive constant. In other words, one of the R values must be specified in order to calculate the others. Since $\rho = \exp(R)$, ρ is determined apart from a multiplicative constant. In order to determine this multiplicative constant it is sufficient to make a single voltage measurement between two points on the boundary. Assume that the reconstructed image $R_{\text{rec}} = R_{\text{true}} + K$ where K is the constant to be determined. Then

$$\rho_{\text{rec}} = k\rho_{\text{true}}$$

where $k = \exp(K)$.

Since integrating the electric field gives us the voltage difference

$$\int_{l_1}^{l_2} \rho_{\text{true}} \mathbf{J} \cdot d\mathbf{l} = V_{12}$$

where $l(x, y, z)$ is a path in Ω connecting the two points on the boundary, l_1 and l_2 are the beginning and end points of this line, V_{12} is the voltage difference between these points and $d\mathbf{l}$ is the differential vector on this line

$$\int_{l_1}^{l_2} k^{-1} \rho_{\text{rec}} \mathbf{J} \cdot d\mathbf{l} = k^{-1} \int_{l_1}^{l_2} \rho_{\text{rec}} \mathbf{J} \cdot d\mathbf{l} = V_{12} \quad \text{and} \quad k = \left(\int_{l_1}^{l_2} \rho_{\text{rec}} \mathbf{J} \cdot d\mathbf{l} \right) / V_{12}. \quad (22)$$

3. Implementation and simulation

2D simulations are made to illustrate the performance of the methods. For a 2D problem it is sufficient to consider the third row of (6) only (for reconstructions in the xy plane). A square resistive object of 20 cm \times 20 cm dimensions, placed in the region ($0 \leq x \leq 20$ cm, $0 \leq y \leq 20$ cm), is uniformly discretized into 50 \times 50 square elements. In order to generate data simulating \mathbf{J} , for an assumed resistivity distribution and injected current profile, FEM is used to calculate the internal current density distribution. For FEM purposes, two triangles are used to form each square, adding up to $2 \times 50 \times 50 = 5000$ triangular finite elements. In a triangular element, resistivity is assumed to be constant, voltage is assumed to be planar, and therefore the current density is also constant. Once current density is calculated for all triangular elements, the average of the current densities for the two triangles encompassed by a square pixel is assigned as the current density value for that pixel. On the right-hand side of equation (15), the derivatives of the current density components appear. To find these derivatives, finite difference approximations using central differences for internal pixels, and forward and/or backward differences at the borders are used in a similar way to that explained in section 2.3. The centre points of the square pixels are the points used for finite difference formulations.

Within the square object, two regions which have conductivities different from the background are assumed. One of the regions, which is of square shape, has resistivity of 0.5 k Ω cm, and the other region, which is of circular shape, has resistivity of 2 k Ω cm (see figure 3). Background resistivity is taken to be 1 k Ω cm. Two ‘injected current profiles’ are used. For the first case, the current is sourced uniformly from the $y = 0$ edge of the 20 cm \times 20 cm square object, and sunk from the $y = 20$ cm edge. For the second case, current is sourced uniformly from the $x = 0$ edge and sunk from the $x = 20$ cm edge. For these two injected current profiles the condition given in equation (17) is satisfied for all points.

In order to observe the conditioning of the inverse problem, singular value decomposition is used to find the singular values of the combined set of equations explained in section 2.3

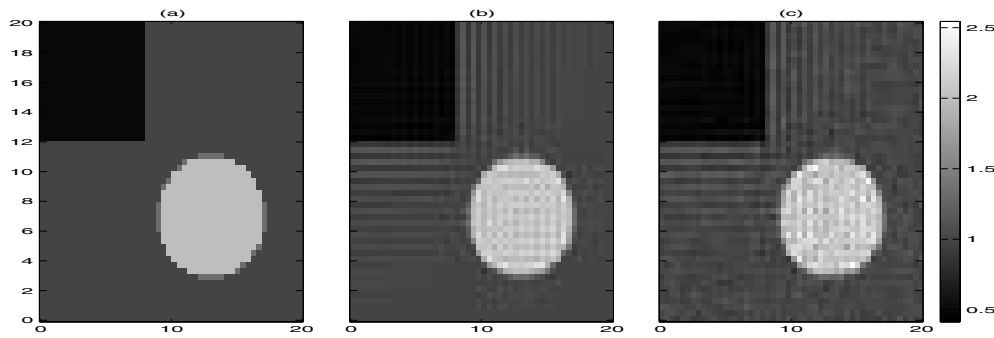


Figure 3. (a) Simulation object with two regions, one square and the other circular, which have resistivities different from the background. (b) Reconstructed image found by solving a linear set of equations, for the simulation object shown on the left. (c) Reconstructed image using the same method but with noisy simulated data.

for $M = 2$. For 50×50 discretization, there are 2500 singular values one of which turns out to be very small; and the remaining singular values have a condition number of 54 (the condition number is the ratio of the largest singular value to the smallest). Since one of the pixel resistivities must be specified anyhow, this result shows that the system is very well conditioned. For a 20×20 discretization of the imaging region there are 400 resistivity pixels. For this case the rank of the system matrix is found to be 399. For the 399 nonzero singular values of this matrix, the condition number is 13. Thus if the discretization is coarser, the system becomes better conditioned while spatial resolution is compromised.

Figure 3 shows the reconstructed image obtained by solving the combined set of equations in the least-squares sense for 50×50 discretization. The value of resistivity at $(x, y) = (0, 0)$, i.e. the resistivity of the left-bottom square pixel, is assumed to be known. The reconstructed image is almost an exact replica of the actual object except for minor fluctuations which can be attributed to the finite difference as well as the FEM approximations. A similar image is obtained when uniformly distributed noise is added to \mathbf{J}^1 and \mathbf{J}^2 . Noise is added to the x and y components of the current density separately. For each pixel, 10% of the magnitude of the corresponding current density component is multiplied by the outcome of a uniform random number generator, which has a range of ± 1 , and the result is added to that current density component. The image obtained with the noisy current densities (see figure 3) indicates that the method is stable against additive noise. This result is also indicative of the fact that an inverse crime is not made. Since the forward solution is calculated using FEM, and the inverse formulation is based on finite differences, the possibility of an inverse crime is further reduced.

For the same simulation object the method of reconstruction by integrating along Cartesian grid lines is also applied, again assuming that $\rho(0,0)$ is known. First $\partial R/\partial y$ is integrated from $(0, 0)$ to $(0, 20)$ to obtain the values of the pixels on the left-hand side of the object. Then starting from these values, pixel values along the x direction are calculated by integrating $\partial R/\partial x$. For integration, the trapezoidal method is used for the 50×50 discretization where the integration points are the centre points of the square pixels. The result is given in figure 4. In this case the small interior square object's edges are reconstructed in a more blurred manner. Also errors made in the first integral bias the R values on a horizontal line. When the reconstruction is repeated for noisy data as explained previously, it is found that the method does not blow up (accumulation of noise effects is not observed) but is stable against noise interference (see figure 4).

Finally, reconstruction along equipotential lines is applied. In figure 5, equipotential lines as well as the current streamlines for the simulated conductivity distribution are shown for

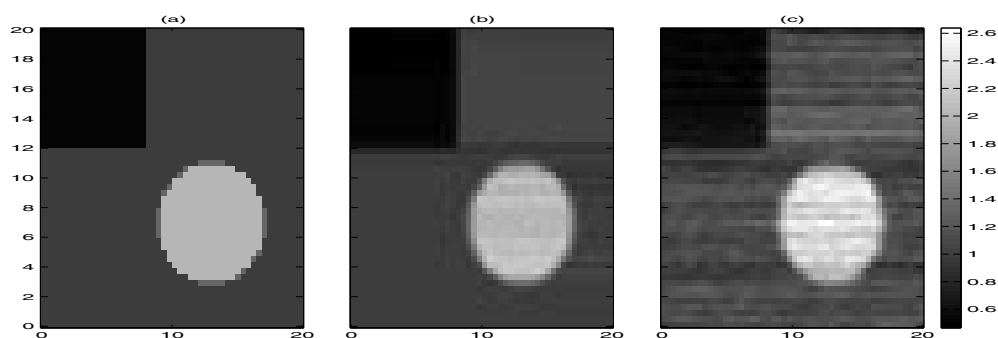


Figure 4. (a) Simulation object with two regions, one square and the other circular, which have resistivities different from the background. (b) Reconstructed image found by integrating along the Cartesian axes, for the simulation object shown on the left. (c) Reconstructed image using the same method but with noisy simulated data.

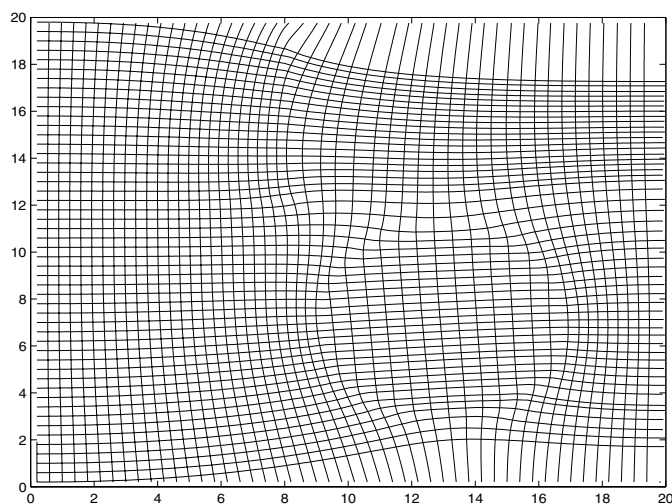


Figure 5. Equipotential lines and current streamlines for the injected current profile for which current is sourced at the $y = 0$ edge, and sunk at the $y = 20$ cm edge.

the case of an injected current profile for which current is sourced at the $y = 0$ cm line and sunk at the $y = 20$ cm line. In general current streamlines run up from the bottom, and the equipotential lines run from left to right as expected. Equipotential lines are calculated starting from the centre points of the pixels which lie on the left edge of the square object, resulting in 50 such lines. In order to reconstruct the resistivity distribution we now assume that values of the pixel resistivities at the $x = 0$ border are known, and equation (13) is evaluated starting from these initial values. The integration step size for s in equations (11) and (13) is taken to be such that the points on the equipotential lines are placed at roughly 1 mm intervals. If a particular square resistivity pixel has certain equipotential points falling in it, then the resistivities calculated at those equipotential points are averaged and the average value is assigned to that pixel. Figure 6 shows the reconstructed resistivity distribution. Those pixels which are not transversed by any of the equipotential lines, cannot be assigned a value.

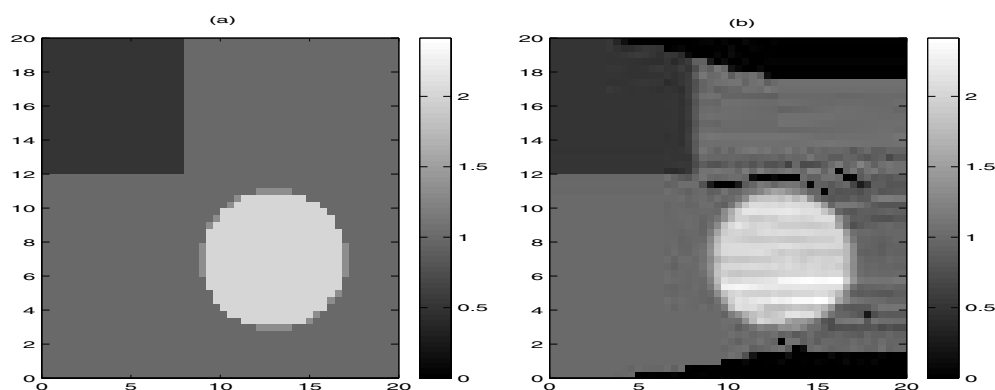


Figure 6. (a) Simulation object with two regions, one square and the other circular, which have resistivities different from the background (b) Reconstructed image found by integrating along equipotential lines, for the simulation object shown on the left. The darkest pixels are those for which resistivity assignment could not be made.

Such pixels are assigned to have zero resistivity so that they show up in figure 6 as the darkest regions.

It is of course possible to generate the equipotential lines with more frequency and from more starting points so that all pixels are transversed. Alternatively an equipotential line can be generated for each pixel passing through the centre point of that pixel. We have chosen to reconstruct with fewer than the necessary number of equipotential lines for the purpose of illustrating this necessity.

It is assumed in this method that the resistivities of the leftmost pixels are known. In order to find the resistivities of those pixels, one can then apply another injected current profile, so that those pixels lie on several equipotential lines for the new injected current profile, thereby reducing the number of unknowns to a fewer number of pixels. In general, with two injected current profiles which satisfy condition (17), it should be possible to reconstruct the whole image except for a single pixel resistivity, by alternatively integrating on equipotential lines of the two injected current profiles.

4. Conclusions and discussion

It has been shown that if the condition given in equation (18) is satisfied for each point in the domain for at least a single pair of injected current profiles, then 3D reconstruction of the resistivity is possible apart from a multiplicative constant. The condition in (18) is an over-specification, as explained in section 2.1. A single voltage measurement is enough to determine the multiplicative constant.

The requirement of condition (18) has been arrived at by the investigators who have developed the J -substitution algorithm as well (see Kwon *et al* (2002b) for a rigorous treatment). The derivation of condition (18) has however been based on completely different and more straightforward grounds in this study.

In many applications the true values of the pixel resistivities may not be required, and only the relative variation of resistivity in the imaging region may be of interest. In such cases there is no need for the additional single voltage measurement to identify the multiplicative constant. This significantly reduces the instrumentation requirements because then only the availability of a current source for current injection suffices.

The methods proposed in this study are applicable to 3D reconstructions in various ways:

- Reconstruction by solving the linear set of equations derived using finite differences can be formulated for the 3D problem.
- Reconstructions can be done for all $z = \text{constant}$ planes (or for all $x = \text{constant}$ or $y = \text{constant}$ planes).
- Reconstruction by integrating along Cartesian axes can be done in all three directions.
- Reconstruction based on integrating along equipotential lines can be done along equipotential lines covering the whole 3D object.

The methods proposed are direct. They require either the inversion of a single well-conditioned matrix or they require integrations along Cartesian or equipotential lines. Furthermore the methods are not iterative.

The methods proposed are not particularly sensitive to noise. The amount of noise added to the simulated current density data is twice that added by Kwon *et al* (2002a) in their simulations of the J -substitution algorithm. In the J -substitution algorithm, the magnitude of \mathbf{J} is used as opposed to the components of current density used in this study. This may have a smoothing effect on the measurement noise. The purpose of noisy simulations in this study is to demonstrate that the algorithms do not have an oversensitivity to noise in the data. For future work, comparison of different algorithms, which have appeared in the MREIT literature so far, with respect to their noise tolerances need be considered. In particular, methods utilizing \mathbf{J} need be compared to methods utilizing \mathbf{H} directly. The reason for this need is that due to the curl operation used in obtaining \mathbf{J} from \mathbf{H} , noise in \mathbf{J} will be more pronounced. Noise studies for MR-EIT algorithms need however be based on a realistic noise model based on the peculiarities of the magnetic resonance system being used for measuring \mathbf{H} . Scott *et al* (1991) have reported a realistic noise model for MRCDI studies and this model has been used in the work of Birgöl *et al* (2003) in simulating their MR-EIT algorithm.

Despite the fact that the method of integration along equipotential lines is difficult to utilize because one needs to generate equipotential lines covering the whole region, it offers an interesting possibility for practical use. If in practice the resistivity of a certain FOV in the object is desired, then only the equipotential lines covering that region need to be evaluated. Khang *et al* (2002) have also discussed this matter with regard to the J -substitution algorithm. Indeed, it is possible to image a certain FOV using the J -substitution algorithm by imposing the measured current density at the boundary of the FOV as a Neumann boundary condition so that the numerical procedures can be applied for that FOV only.

Scott *et al* (1991) have also made use of the identity, $\nabla \times \rho \mathbf{J} = 0$, in verifying their MRCDI methods. They have not, however, developed algorithms for MR-EIT by utilizing this identity. Seo *et al* (2002) have made use of the fact that the curl of the electric field vanishes in the domain, in developing their MR-EIT algorithm which makes use of a single component of the magnetic field.

The method of characteristics has been applied to many inverse problems of practical interest. For the interested reader we can cite the work of Richter (1981) who has applied the method to the problem of rock permeability reconstruction which arises in groundwater flow studies.

Appendix

R can be found completely on an equipotential surface, if it is specified at single point on it. One method is to first find R on the characteristic curve, L , passing from the specified point, obtained using one of the rows of the hyperbolic system in (6). Then, starting from points

on L , we complete the equipotential surface along characteristic curves of either one of the remaining rows of the hyperbolic system. L is a non-characteristic curve for the equipotential surface in the complete sense, i.e. it intersects all characteristic curves of either one of the remaining rows of the system. This completes the determination of R .

The other method is to find R at any other point in the equipotential surface by integrating along any path in the surface starting from the specified point. For the hyperbolic system

$$\tilde{\mathbf{J}}^T \nabla R = \mathbf{b} \quad (23)$$

where $\mathbf{b} = -\nabla \times \mathbf{J}$, and let $\underline{\mathbf{x}}(s)$ be a curve on a characteristic surface joining the point we are interested in to $\underline{\mathbf{x}}(s_0)$ where R is known. Since $\underline{\mathbf{x}}(s)$ is on the characteristic surface, $\mathbf{x}'(s) \in \text{Range}(\tilde{\mathbf{J}}_i(s))$, $i = 1, 2, 3$ and $\mathbf{x}'(s) \neq 0$. Hence there is a nonzero vector field $\underline{\mathbf{c}}(s)$ along $\underline{\mathbf{x}}(s)$ such that

$$\mathbf{x}'(s) = \tilde{\mathbf{J}}(\mathbf{x}(s))\underline{\mathbf{c}}(s). \quad (24)$$

Now, $\underline{\mathbf{c}}^T \tilde{\mathbf{J}}^T \nabla R = \underline{\mathbf{c}}^T \mathbf{b}$ along the curve $\underline{\mathbf{x}}(s)$, and hence $(\tilde{\mathbf{J}}\underline{\mathbf{c}}) \nabla R = \underline{\mathbf{c}}^T \mathbf{b}$, and $\mathbf{x}'(s) \nabla R = \underline{\mathbf{c}}^T \mathbf{b}$. Therefore,

$$R(\underline{\mathbf{x}}(s)) = R(\underline{\mathbf{x}}(s_0)) + \int_{s_0}^s (\underline{\mathbf{c}}^T \mathbf{b})(\underline{\mathbf{x}}(t)) dt. \quad (25)$$

References

- Birgöl Ö, Eyüboğlu B M and İder Y Z 2003 Current constrained voltage scaled reconstruction (CCVSR) algorithm for MR-EIT and its performance with different probing current patterns *Phys. Med. Biol.* **48** 653–71
- Eyüboğlu M, Birgöl Ö and İder Y Z A 2001 Dual modality system for high-resolution true conductivity imaging *XIth Int. Conf. Electrical Bioimpedance (ICEBI) (Oslo, Norway)* 409–13
- Eyüboğlu B M, Reddy R and Leigh J S 2002 Magnetic resonance–electrical impedance tomography *Patent* no US 6,397,095 B1, provisional patent application on Mar. 1 1999
- İder Y Z and Birgöl Ö 1998 Use of magnetic field generated by the internal distribution of injected currents for electrical impedance tomography (MR-EIT) *Elektrik Turkish J. Elec. Eng. Comput. Sci.* **6** 215–25
- İder Y Z and Müftüler T 1997 Measurement of ac magnetic field distribution using magnetic resonance imaging *IEEE Trans. Med. Imaging* **16** 617–22
- John F 1982 *Partial Differential Equations* (Berlin: Springer)
- Khang H S, Lee B I, Oh S H, Woo E J, Lee S Y, Cho M H, Kwon O, Yoon J R and Seo J K 2002 J -substitution algorithm in magnetic resonance electrical impedance tomography (MREIT) phantom experiments for static resistivity images *IEEE Trans. Med. Imaging* **21** 695–702
- Kim S, Kwon O, Seo J K and Yoon J-R 2002 On a nonlinear partial differential equation arising in magnetic resonance electrical impedance tomography *SIAM J. Math. Anal.* **34** 511–26
- Kwon O, Lee J-Y and Yoon J R 2002b Equipotential line method for magnetic resonance electrical impedance tomography *Inverse Probl.* **18** 1089–100
- Kwon O, Woo E J, Yoon J-R and Seo J K 2002a Magnetic resonance electrical impedance tomography (MREIT): simulation study of J -substitution algorithm *IEEE Trans. BME* **49** 160–7
- Özdemir M and Eyüboğlu B M 2002 Novel fast reconstruction algorithm for magnetic resonance electrical impedance tomography *Proc. Biyomut 8th Annual Conf. (Istanbul, Turkey)* (CD-ROM)
- Richter G R 1981 An inverse problem for the steady state diffusion equation *SIAM J. Appl. Math.* **41** 210–21
- Scott G C, Joy M L G, Armstrong R L and Hankelman R M 1991 Measurement of non-uniform current density by magnetic resonance *IEEE Trans. Med. Imaging* **10** 362–74
- Seo J K, Kwon O, Yoon J-R, Lee B I and Woo E J 2002 Single component of magnetic flux density can produce resistivity images in magnetic resonance electrical impedance tomography (MREIT) *First Mummy Range Workshop on Electrical Impedance Imaging (Pingree Park, CO)* abstract
- Sylvester J and Uhlmann G 1986 A uniqueness theorem for an inverse boundary value problem in electrical prospection *Commun. Pure Appl. Math.* **17** 91–112
- Woo E J, Lee S Y and Mun C W 1994 Impedance tomography using current density distribution measured by nuclear magnetic resonance *SPIE* **2299** 377–85
- Zhang N 1992 Electrical impedance tomography based on current density imaging *MSc Thesis* University of Toronto